PROCEEDINGS A

royalsocietypublishing.org/journal/rspa

Research

Cite this article: Carmigniani R, Seifert L, Chollet D, Clanet C. 2020 Coordination changes in front-crawl swimming. *Proc. R. Soc. A* **476**: 20200071.
http://dx.doi.org/10.1098/rspa.2020.0071

Received: 4 February 2020
Accepted: 5 March 2020

Subject Areas:
biomechanics, fluid mechanics

Keywords:
motor coordination, burst-and-coast, front-crawl swimming

Author for correspondence:
R. Carmigniani
e-mail: remi.carmigniani@enpc.fr

Electronic supplementary material is available online at https://doi.org/10.6084/m9.figshare.c.4950921.

THE ROYAL SOCIETY PUBLISHING

Coordination changes in front-crawl swimming

R. Carmigniani[1], L. Seifert[2], D. Chollet[2] and C. Clanet[3]

[1]LHSV, Ecole des Ponts, CEREMA, EDF R et D, Marne-la-Vallee, France
[2]CETAPS EA3832, Faculty of Sports Sciences, University of Rouen Normandy, Mont-Saint-Aignan, France
[3]LadHyX, Ecole Polytechnique, Palaiseau, France

RC, 0000-0001-6456-9624; CC, 0000-0003-2448-0443

We report the evolution of the coordination with velocity in front-crawl swimming which is used in competitions over a large range of distances (from 50 m up to 25 km in open-water races). Inside this single stroke, top-level swimmers show different patterns of arm organization. At low velocities, swimmers select an alternated stroke with gliding pauses during their propulsion. The relative duration of the gliding pauses on a stroke cycle is independent of the velocity in this first regime. Above a critical velocity, the relative duration of the gliding pauses starts to decrease as speed increases. Above a second critical velocity, the gliding pauses disappear and the swimmers start to superpose their propulsion phases. These three regimes are first revealed experimentally and then studied theoretically. It appears that below the first critical velocity, swimmers use a constant coordination index and vary their speed by varying their propulsive force to minimize their cost of propulsion. For larger velocities, swimmers use their maximum propulsive force and vary their recovery time to increase further their speed. The physical model developed is general and could be applied to understand other modes of locomotion.

1. Introduction

Although we can find evidence of swimming in the fossils and tools of Neanderthals well before the arrival of modern humans in Western Europe [1–3], modern competitive swimming started in early nineteenth-century England [4]. The search for speed in swimming led to changes in the technique from the natural quadruped dog fashion technique to the breaststroke, then sidestroke and Trudgen stroke, all the way to the

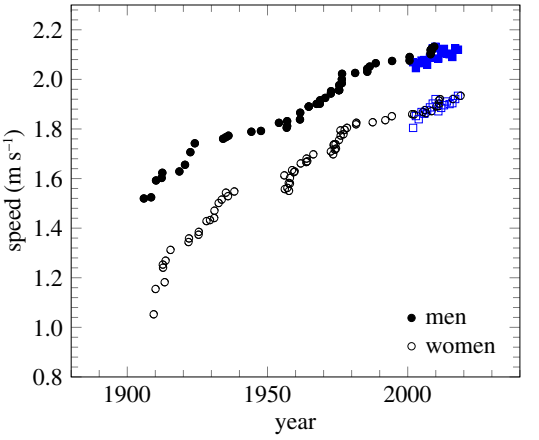

Figure 1. Evolution of the mean velocity over time of the 100 m long course freestyle. The circles denote world record evolution. The blue squares denote the year best performance from 2001 to today. (Online version in colour.)

modern front-crawl. The front-crawl was pioneered in competition by the Australian Richard Cavill at the beginning of the twentieth century. He was largely inspired by native surfers from the Solomon Islands [4]. The technique was refined over time as the average speed of swimmers continued to increase over the century (figure 1).

Front-crawl swimming is now used in a large range of distances in swimming pool and open-water races. It appears to be the most efficient swimming technique as it is the only one used for long distances (over 200 m) and the fastest one (used in freestyle sprint) [5]. It is characterized by alternated arm propulsion phases in the water and arm recovery out of the water. The frequency of an arm cycle is often called stroke rate (f_R). Swimmers can vary their stroke frequency for a given mean velocity ($\overline{v}$). Researchers observed that swimmers did not use the minimum stroke rate they could achieve for long-distance races (over 200 m), suggesting they will not use their highest force per stroke [6,7].

To understand this frequency–velocity choice, researchers looked at arm organization during a cycle [8,9]. They found that inside this single stroke, swimmers show different organization. At low velocities, swimmers select an alternated stroke with gliding pauses in between their propulsion phases. This is represented schematically in figure 2. The shaded grey blocks show the propulsive phases during a stroke cycle. The gap between two propulsive phases represents the duration during which the swimmer is gliding. During this glide they adopt a streamline arm position as illustrated in figure 2*b*. This pattern of arm organization is called the *catch-up* mode. The repartition of gliding pauses on a stroke cycle ($|t_c|/T$) varies with velocity [10]. Researchers found that the ratio $|t_c|/T$ decreases slowly with an increase of pacing velocity corresponding to long races (from 1500 m, 800 m to 400 m races) and decreases more rapidly for higher velocities (from the 200 m race pace to the 50 m). This seems to separate sprint paces (50 m and 100 m races) from distance paces (400 m, 800 m and 1500 m races).

In the high-velocity regime (sprint paces), the gliding pauses disappear rapidly as velocity increases and some elite swimmers are even able to superpose their propulsion phases taking advantage of a fast air recovery (figure 3) [10]. This new pattern is called the *superpositon* mode. For elite swimmers, this change from catch-up to superposition mode occurs above 1.7–1.8 m s^{-1}. Up to the authors knowledge, a physical approach to explain the general evolution of the stroke with speed has not yet be presented.

In the present paper, we look at how swimming coordination varies with speed. In §2, we present the on-field observations and define the index of coordination. A first physical model on coordination is detailed in §3 prior to the burst-and-coast approach presented in §4. Applications and perspectives are given in §5.

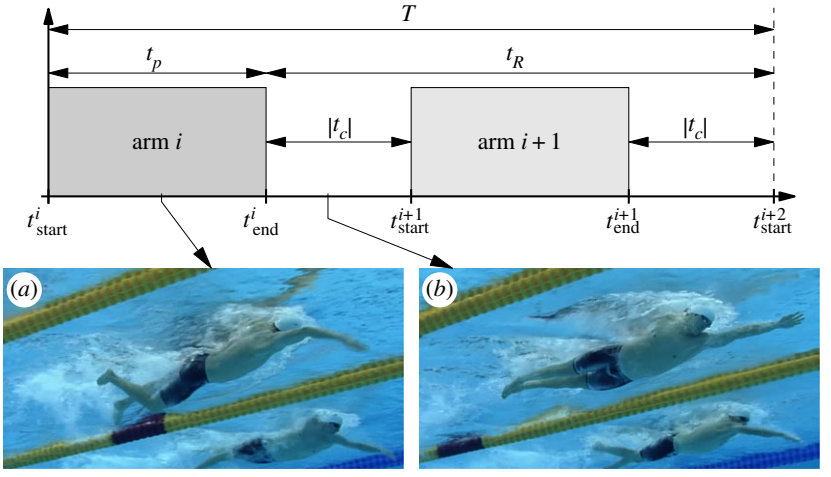

Figure 2. Catch-up mode of coordination. A stroke cycle lasts a period T. During a cycle, swimmers alternate two propulsion phases (shaded grey blocks) with gliding pauses in between. The duration of the gliding pauses is denoted $|t_c|$. A single arm is generating a thrust during time t_p and recovers during t_R. Photos are extracted from races at the Olympic Games with the permission of The Olympic Multimedia Library. (Online version in colour.)

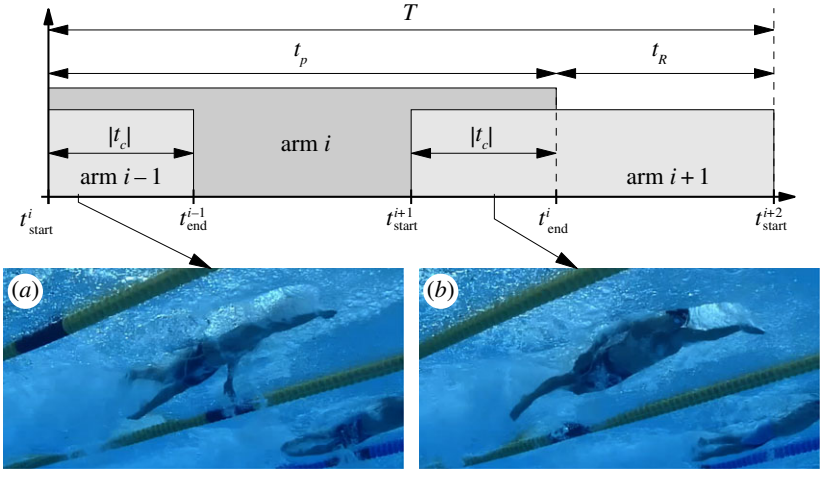

Figure 3. Superposition mode of coordination. A stroke cycle lasts a period T. During a cycle, swimmers alternate two propulsion phases (shaded grey blocks) with superpositions of propulsion (overlapping shaded blocks). The duration of the superposition period is denoted $|t_c|$. A single arm is generating a thrust during time t_p and recovers during t_R. Photos are extracted from races at the Olympic Games with the permission of The Olympic Multimedia Library. (Online version in colour.)

2. Definitions and observations

(a) Index of coordination

Swimmers alternate propulsion phases with their two arms in the catch-up (figure 2) and superposition (figure 3) modes. To simplify the discussion, we assume both arms are identical and a stroke cycle periodic. One arm performs a full cycle in a period $T = t^{i+2}_{\text{start}} - t^i_{\text{start}}$, generates a propulsive force during a time $t_p = t^i_{\text{end}} - t^i_{\text{start}}$ and recovers during the rest of the cycle, t_R. We

Table 1. Swimmer information. LC stands for long course. NPW is the number of practice per week. YP is the number of year of practice confirming their expert level [11].

parameters	mean ± s.d. (min,max)	parameters	mean ± s.d. (min,max)
age	21.2±4.4 (19,31) years	body mass	78.8±8.5 (66.3,90.5) kg
height	1.84 ± 0.03 (1.70,1.93) m	arm span	1.91 ± 0.08 (1.70,2.14) m
arm length	0.65±0.05 (0.60, 0.75) m	YP	12.1±3.5 (7,20) years
NPW	9.0± 1.8 (5,10)	100-m (LC)	54.2 ±1.8 (50.33, 57.8) s

define the coordination time $t_c = t^i_{\text{end}} - t^{i+1}_{\text{start}}$ and the index of coordination

$$\text{IdC} = \frac{t_c}{T}. \tag{2.1}$$

The catch-up mode is defined by $\text{IdC} < 0$ while $\text{IdC} > 0$ represents the superposition mode. The special case $\text{IdC} = 0$, where the recovery time is exactly equal to the propulsion time is called opposition mode. Note that with these conventions, $T = t_p + t_R = 2(t_p - t_c)$ and thus $\text{IdC} = t_p/T - 1/2$.

(b) Field measurements: drag and coordination

Following the work of Chollet *et al.* [9], we consider the motor coordination of 16 national level French swimmers (table 1). To focus solely on the arm coordinations, the swimmers legs are tied and they are equipped with a pull buoy to avoid legs sinking.

Each swimmer performed two graded speed tests in a randomized order using only the arms in front-crawl. In the following, we selected three swimmers (M1 to M3) to illustrate the measurement methods and results.

The first test aimed at characterizing swimmer water resistance. To this end, we used the so-called MAD (measure the active drag) system [12–14]. In this test, the swimmers push off from fixed pads spaced 1.35 m and 0.8 m below the water surface with each stroke. This enables one to estimate the total mean drag force assuming constant mean swimming velocity. All the swimmers were tested at 10 different speeds on the MAD system.

Figure 4*a* shows the obtained results for the three selected swimmers. The drag force is fitted to $\overline{D}_b = k_b^{\text{MAD}}\overline{v}^2$ to estimate the total body drag coefficient. For the current three swimmers, the values range from $k_b^{\text{MAD}} = 24.8 \pm 0.8$ to $38.0 \pm 0.9\,\text{kg m}^{-1}$. The error bars correspond to the standard errors for the parameter estimate of k_b^{MAD} fitted. The mean value on the 16 swimmers is $30\,\text{kg m}^{-1}$.

The second test consists of simulated racing techniques where these expert swimmers were asked to swim at eight different velocities corresponding to different race paces (from 3000 m to 50 m + maximal speed) on a single 25 m lap. During this test, the swimmers were video recorded by two synchronized underwater video cameras at 50 fps (Sony compact FCB-EX10L), in order to get a front and side view, from which the different stroke phases and the arm coordination have been computed. The protocol is similar to the one described in [9,10,14]. Three expert operators are used to analyse the key points of the arm stroke with a blind technique, that is without knowing the analyses of the other two operators. This leads to absolute error on the index of coordination of 3% [15]. The mean velocity is evaluated using an external side-view video camera recording at 50 fps on a distance of 12.5 m. The relative error of the mean velocity is 1%.

Figure 4*b* shows examples of the evolution of the index of coordination with the mean velocity $\overline{v}$ for the three swimmers. Overall, it is observed that the swimmers tend to increase their coordination index as they increase their velocity changing from a catch-up to a superposition mode. The swimmer M3 reaches a superposition mode for his two highest velocities. The maximum mean velocities of the swimmers M1 and M2 are close to $1.5\,\text{m s}^{-1}$ but yet their

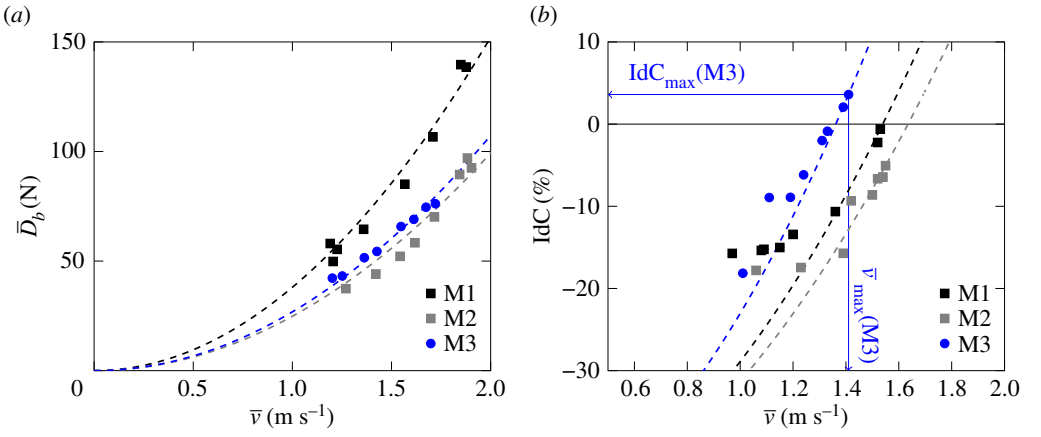

Figure 4. (*a*) Body drag estimated with the MAD system with the mean velocity for three swimmers. The dashed lines correspond to the fitted curve $\overline{D}_b = k_b^{\mathrm{MAD}}\overline{v}^2$. (*b*) Evolution of the index of coordination (IdC) with the mean velocity for the same swimmers. The dashed lines correspond to $\mathrm{IdC} = 1/2(\overline{v}/v^*)^2 - 1/2$ with $\widetilde{v} = v^*$ where $v^* = \overline{v}_{\mathrm{max}}/\sqrt{1 + 2\mathrm{IdC}_{\mathrm{max}}}$ and $\overline{v}_{\mathrm{max}}$ and $\mathrm{IdC}_{\mathrm{max}}$ are the mean velocity and index of coordination of the fastest trial for each swimmer read as shown for M3. (Online version in colour.)

coordination patterns are different, respectively −0.5% and −5%. On the other hand, it can be seen that swimmers M3 and M1 are close to the opposition mode (IdC = 0) for drastically different velocities. At lower velocities, these three swimmers choose similar coordination patterns. Swimmers M2 and M1 show a flattening of the evolution of their index of coordination with velocity. This is not observed for swimmer M3. This outlines the individualization of the technique.

3. First coordination model

Writing Newton's Second Law on the swimmer system in the direction of the race, we get

$$m_0 \frac{\mathrm{d}v}{\mathrm{d}t} = T_b - D_b, \tag{3.1}$$

where m_0 is the mass of the swimmer plus some added mass of the water, v is the instantaneous velocity, T_b the total instantaneous thrust generated by the swimmer and D_b the body drag. Averaging on a stroke cycle and assuming a periodic regime is reached, it becomes

$$0 = \overline{T}_b - k_b\overline{v}^2, \tag{3.2}$$

where we assumed $\overline{D}_b \approx k_b\overline{v}^2$ and the overline denotes the average on a cycle. For instance, for a quantity a: $\overline{a} = 1/T\int_0^T a(t)\,\mathrm{d}t$. The approximation in $\overline{D}_b$ comes from the fact that we neglect the velocity fluctuations in the drag evaluation. As typical velocity fluctuations of swimmers in front-crawl are of the order of 13% of the mean velocity [16], this is a good approximation and in the remainder we will replace the approximation by an equal sign for brevity. In §4, this approximation is relaxed.

We can further separate the thrust of each arm and define $T_a^i(t)$ as the instantaneous thrust of arm i at t. In this simplified symmetrical model, during a cycle, the two arms will produce the same mean thrust and thus we can define

$$\widetilde{T}_a = \frac{1}{t_p}\int_0^{t_p} T_a\,(t)\,\mathrm{d}t, \tag{3.3}$$

where $\widetilde{T}_a$ denotes the mean thrust generated by one arm during propulsion. It is reasonable to assume that this thrust can be controlled by the swimmer and is bounded, $\widetilde{T}_a \in [0, T_a^*]$. T_a^*

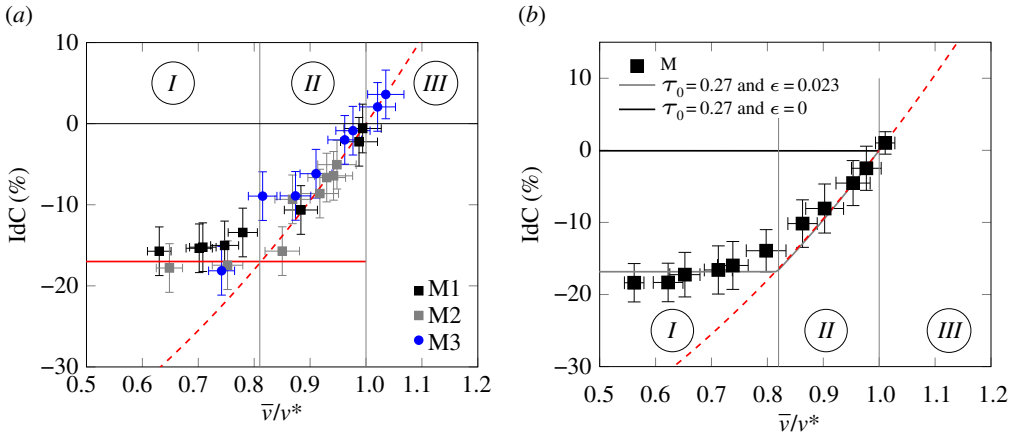

Figure 5. (*a*) Arm coordination with the non-dimensional mean velocity for three swimmers of the data set. The dashed line corresponds to equation (3.5). The horizontal solid red line is a guide for the eyes outlining the plateau the swimmers seem to converge towards at low velocities. Three regimes are observed: *I*, a low-velocity regime where the IdC is constant; *II*, a transitional regime from catch-up mode to superposition where the IdC increases with the velocity following the maximum force model and *III* a superposition regime. (*b*) Arm coordination with the mean non-dimensional velocity for the 16 swimmers of the dataset. The dashed line corresponds to the maximum force model. The solid lines show the optimal coordination with $\tau_0 = 0.27$ and $\epsilon = 0$ and $\epsilon = 0.023$ in black and grey, respectively. (Online version in colour.)

corresponds to the maximum thrust they can generate. Injecting this in equation (3.2), we get

$$0 = \frac{2t_p}{T}\widetilde{T}_a - k_b\overline{v}^2. \tag{3.4}$$

Using the relation that $2t_p/T = 1 + 2\text{IdC}$, we then find a relationship between the coordination index and the mean velocity, which depends on the mean thrust generated by one arm during its propulsive phase and the body drag

$$\overline{v} = \widetilde{v}\,(1 + 2\text{IdC})^{1/2}, \tag{3.5}$$

where $\widetilde{v} = \sqrt{\widetilde{T}_a/k_b}$. It can be assumed that at the maximum velocity of the previous coordination test (figure 4*b*) the expert swimmers used their maximum thrust T_a^* to produce their highest speed. Defining $v^* = \sqrt{T_a^*/k_b}$, it becomes

$$v^* = \frac{\overline{v}_{\max}}{\sqrt{1 + 2\text{IdC}_{\max}}}, \tag{3.6}$$

where the index 'max' denotes the test with maximum velocity for each swimmer. The dashed lines in figure 4*b* correspond to equation (3.5) with $\widetilde{v} = v^*$ and is referred to as the 'maximum force model'. The three swimmers nicely follow the model of maximum force when their velocity increases (see red dashed line in figure 5*a*). Calculation of the error bars are detailed in Appendix A. The characteristic velocity, v^*, defined by equation (3.6), is a good estimate of the observed change from catch-up to superposition mode (from *II* to *III* in figure 5*a*). During this change of regime the swimmers mostly reduce their recovery time t_R taking advantage of the low air resistance.

It is further observed that as the swimmers simulate longer races (lower velocities), they tend to diverge from this simple maximum force model. They seem to select a speed-independent coordination pattern (IdC) at low velocity (see red solid line and region *I* in figure 5*a*). Therefore, we define three regimes. At low velocities, there exists a catch-up mode regime with constant index of coordination (regime *I*). Above a first critical velocity $\overline{v} \approx 0.8v^*$, the IdC starts to evolve with the velocity in the catch-up mode (regime *II*) towards the last regime above $\overline{v} \approx v^*$ where the swimmers start to superpose their propulsion (regime *III*).

We apply the same analysis to the 13 other swimmers tested. In all the cases, we use their maximum velocity to define their characteristic velocity v^* using equation (3.6). We group the swimmers in pools of similar $\overline{v}/v^*$ with steps of 0.05 and averaged their coordination index. Each pool contains at least six points and six different swimmers. On average, there are 24 observations per pool with 12 different swimmers. The results are displayed in figure 5*b*. This figure is one of the main results of the present paper. The data are also provided in Appendix B for each of the swimmers. These expert swimmers follow nicely the maximum force model for non-dimensional velocity higher than 0.8 (regime *II* and *III*). Below this value, the index of coordination is almost constant and near a value of [−15%, −20%] (regime *I*).

A similar change of IdC evolution (regime *I* and *II*) at low velocities has been observed within the catch-up coordination pattern at the 200m race pace in previous studies [10,17,18]. Indeed, Seifert *et al.* [10] showed a change of IdC evolution occurred at the 200 m race pace, as this effort separates the sprint paces (50 m and 100 m races) from the distance paces (400 m, 800 m and 1500 m races). A recent study especially focused on the relationships between IdC, energy cost, propelling efficiency within the 200 m race and confirmed the positive correlation between IdC and energy cost, and the negative correlation between IdC and the propelling efficiency [19]. The effect of small variations of speed near the 200 m race pace on IdC has been investigated through an incremental 7 × 200 m test, exhibiting an inflection of IdC and lactate concentration, at the fourth 200 m [19]. In this study, the increase of IdC was also positively correlated with the increase of energy cost of locomotion [20]. This suggests that the change in IdC evolution from regimes *I* and *II* can be linked to an energetic argument. We discuss this change in coordination evolution in the next section using a physical approach.

4. Burst-and-coast in catch-up mode

(a) Physical model

It is interesting to see that at low velocities, swimmers select a coordination pattern which alternates propulsion phases with gliding phases with one arm extended forward. This seems similar to the burst-and-coast swimming behaviour observed for certain fish such as cod or saithe. A model to explain this behaviour was proposed by Videler & Weihs [21]. They found that if the fish had a reduced drag during the gliding phase they could consume less mechanical energy to maintain the same average velocity than in steady swimming. The extended arm during the gliding phases in front-crawl can be interpreted as a way to reduce the body drag [22]. This motivates the present model.

The main assumption in the model is that the resistance is not the same during active and passive swimming. During active swimming, the water resistance will be assumed to have the form $D_b = k_b v^2$ and the swimmer produces a thrust T_b, which will be considered constant (in order to keep the model simple). For the gliding phase, the swimmers have one arm forward fully extended (similarly to the figure 2*b*). The drag is considered to be reduced and $D_b = (1-\epsilon)k_b v^2$, where $\epsilon \geq 0$ during this phase. Bulgakova & Makarenko [22] evaluated the drag difference between different body positions. The difference between the drag with the two arms along the body and one arm extended forward is a good first approximation of the maximum value of ϵ. From their observations, this gives $0 < \epsilon < \epsilon_{\max}$ with $\epsilon_{\max} \approx 9\%$.

As the stroke is supposed to be periodic and the two arms symmetrical, we limit the study to half a stroke cycle. In other words, we focus on a single arm. The swimmer velocity oscillates between two extreme values denoted v_- and v_+. To non-dimensionalize the problem, we define $\tau = t/\tau^*$, $u = v/v^*$ and $\varphi = T_a/T_a^*$, where τ^*, v^* are the characteristic time and velocity defined by

$$\tau^* = \frac{m_0}{k_b v^*} \tag{4.1}$$

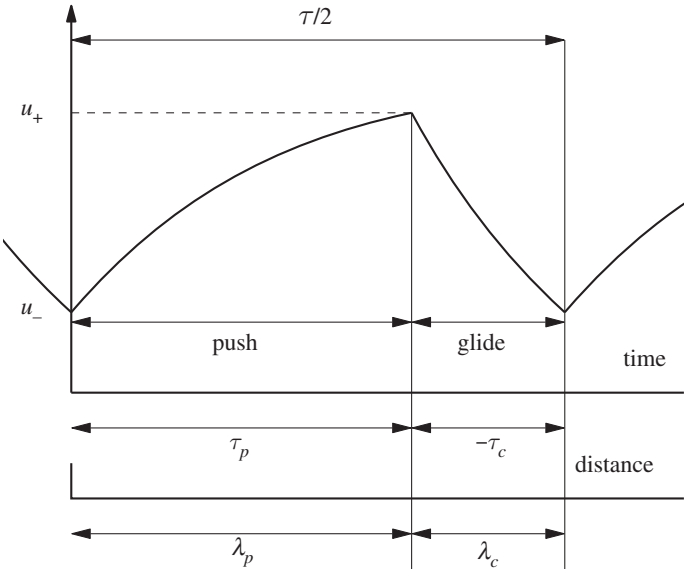

Figure 6. Burst-and-coast model for swimmers intra-cycle velocity variations and notations. (Online version in colour.)

and

$$v^* = \sqrt{\frac{T_a^*}{k_b}}. \tag{4.2}$$

Note that v^* is the same as the one defined in the previous section. Recall that m_0 is the mass of the swimmer plus some added mass. The total mass m_0 is estimated to be $m_0 = (1 + c_a)m_s$, where m_s is the swimmer body mass and $c_a = 0.25 \pm 0.04$ [23,24]. Using these definitions, we write the dynamic equation as

$$\frac{\mathrm{d}u}{\mathrm{d}\tau} = \varphi - u^2, \quad 0 \le \tau \le \tau_p \tag{4.3}$$

and

$$\frac{\mathrm{d}u}{\mathrm{d}\tau} = -(1-\epsilon)u^2, \quad \tau_p \le \tau \le \frac{\mathcal{T}}{2}, \tag{4.4}$$

with boundary conditions

$$u(0) = u\left(\frac{\mathcal{T}}{2}\right) = u_- \tag{4.5}$$

and

$$u(\tau_p) = u_+. \tag{4.6}$$

Figure 6 shows half a cycle with the different notations.

One of the main motivations behind this simple model is that it can be solved analytically. It is rather simple to show that

$$u_+ = \sqrt{\varphi}\tanh\left[\tau_p\sqrt{\varphi} + \tanh^{-1}\left(\frac{u_-}{\sqrt{\varphi}}\right)\right], \quad \tau_c = \frac{1 - u_+/u_-}{(1-\epsilon)u_+} \tag{4.7}$$

and

$$\lambda_p = \log\left(\sqrt{\frac{1 - u_-^2/\varphi}{1 - u_+^2/\varphi}}\right), \quad \lambda_c = \frac{1}{1-\epsilon}\log\left(\frac{u_+}{u_-}\right), \tag{4.8}$$

where λ_p (λ_c) is the non-dimensional distance travelled during the propulsive (gliding) phase (respectively). The mean velocity can be evaluated as $\overline{u} = (\lambda_p + \lambda_c)/(\tau_p - \tau_c)$.

Then the objective of expert swimmers is to swim a given distance as fast as possible. To achieve this goal for long-distance races, they have to control their energy consumption and the problem becomes equivalent to maximizing the distance for a fixed mean velocity. They select the coordination technique that enables them to save the most total energy at this fixed mean velocity. Here, we assume that the total energy cost is proportional to the mechanical cost of swimming similarly to [21]. Therefore, the optimal technique at a given mean velocity is the one that minimizes the energy during a stroke cycle.

The energy consumed during catch-up mode is the energy expended solely during the propulsion phase

$$\mathcal{E}_{\mathrm{cu}} = \int_0^{\tau_p} \varphi u \, \mathrm{d}\tau = \varphi \lambda_p. \tag{4.9}$$

For this amount of energy, the swimmers travel a non-dimensional distance $\lambda_p + \lambda_c$. To travel the same distance in opposition mode (steady swimming), they would use

$$\mathcal{E}_{\mathrm{op,cu}} = \int_0^{\mathcal{T}/2} \overline{\varphi}\, \overline{u} \mathrm{d}\tau = \overline{\varphi}\left(\lambda_p + \lambda_c\right), \tag{4.10}$$

where $\overline{\varphi}$ is the thrust required to swim at the constant velocity $\overline{u} = \sqrt{\overline{\varphi}}$ using equation (4.3). The economy can, therefore, be defined as

$$\mathcal{R}_{\mathrm{cu}} = \frac{\mathcal{E}_{\mathrm{cu}}}{\mathcal{E}_{\mathrm{op,cu}}} = \frac{\varphi}{\overline{u}^2} \frac{\lambda_p}{\lambda_p + \lambda_c}. \tag{4.11}$$

It represents the mechanical energy saved by selecting a catch-up technique over the opposition technique. The swimmer should select the minimum economy. Note that in superposition mode, the economy is always larger than 1. Therefore, for $\overline{u} < 1$ the swimmer should at worst prefer the opposition mode. Above $\overline{u} > 1$, superposition is the only possible mode of coordination.

To solve the problem, we need to add an assumption on the propulsion phase duration, τ_p. We suppose in the next section that it is limited by the arms dynamic.

(b) Propulsion time assumption

In human front-crawl swimming, the propulsion phase duration corresponds to the time the hand needs to travel from the fully extended forward position to the release from the water near the hips. To estimate this time of propulsion, we will simplify the arm+hand to a simple paddle, which travels twice the arm length on a straight line at constant velocity (we neglect the acceleration phases). The thrust generated by the swimmer solely comes from this paddle. The propulsion time is then $\tau_p \approx 2\lambda_a/u_{h/b}$, where λ_a is the non-dimensional arm length and $u_{h/b}$, the non-dimensional hand velocity in the body frame. As the hand+arm travels much faster than the body through the water, we neglect the contribution of the body velocity. We then expect the propulsion time to be of the order of $\tau_p \approx 2\lambda_a/u_{h/w}$, where $u_{h/w}$ is the hand velocity with respect to the water. This velocity depends on the resistance coefficient of the hand $\alpha_h = k_h/k_b$ and the force used by the swimmer to move it through the water: $\alpha_h u_{h/w}^2 = \varphi$, and therefore

$$\tau_p \approx \frac{\tau_0}{\sqrt{\varphi}}, \tag{4.12}$$

where τ_0 is a characteristic time of propulsion. It depends on the arm length λ_a and the α_h coefficient

$$\tau_0 \approx 2\lambda_a \sqrt{\alpha_h}. \tag{4.13}$$

The propulsion time increases with the arm length (larger distance to travel) and the hand size (α_h increases). Note that it does not depend on the swimmer's force. Using the dimensional parameters, we get $\tau_0 \approx 2L_a\sqrt{k_h k_b}/m_0$, with $L_a = 0.52\,\mathrm{m}$ the arm length, $m_0 \approx 1.25 \times 80\,\mathrm{kg}$, $k_h \approx 24\,\mathrm{kg/m}$ the drag coefficient of the hand+arm [25–27] and $k_b = 30\,\mathrm{kg/m}$. This gives $\tau_0 \approx 0.28$.

To check this assumption, we look at the propulsion time of our 16 swimmers. If it is correct, we should observe a constant propulsion time in regimes *II* and *III*. In these regimes, the swimmers

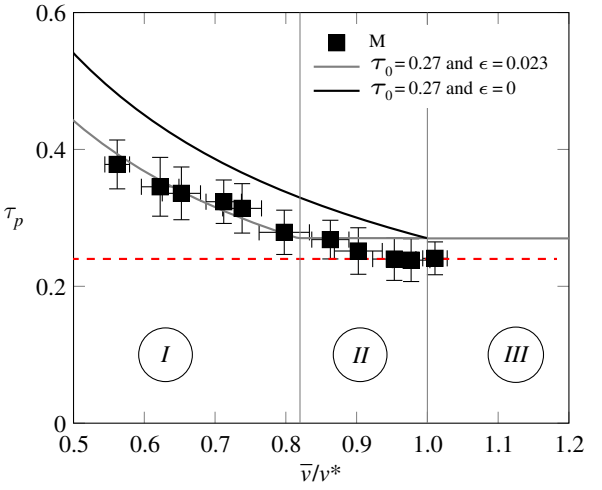

Figure 7. Non-dimensional propulsion time of expert swimmers with the non-dimensional mean velocity. The dashed red line shows the evaluation of the τ_0 based on the observations. The solid lines show the optimal propulsion time with $\tau_0 = 0.27$ and $\epsilon = 0$ and $\epsilon = 0.023$ in black and grey, respectively. (Online version in colour.)

are at their maximum force and $\varphi = 1$ in our model. We can evaluate the propulsion time as $\tau_p = t_p/\tau^*$. Figure 7 shows the obtained mean value of the non-dimensional propulsion phases with the non-dimensional velocity. We see that the propulsion time decreases with velocity and plateaus to $\tau_0 = 0.24 \pm 0.02$ when the points are on the maximum force model in figure 5*b* (four last points in regime *II*). This value is in good agreement with the previous scaling.

(c) Comparison to the dataset

To summarize, the swimmers are characterized by two parameters: the propulsion time parameter τ_0 and the gliding effectiveness ϵ. Both parameters could be measured on swimmers. To minimize their propulsion cost at a given mean velocity, they can play on their force used to produce the thrust $\varphi \in [0, 1]$. We can write this problem in the form

$$\min_{\varphi,\ \text{s.t. } \overline{u}=u_0} \mathcal{R}_{\text{cu}}(\varphi)\,. \tag{4.14}$$

This problem can be solved and would yield the optimal coordination index for our model swimmer for a given mean velocity $\overline{u} = u_0$.

To compare the present burst-and-coast model to our dataset, we used Powell's conjugate direction method [28] with a golden-section search [29] on ϵ and τ_0 to minimize the error on the model prediction on the index of coordination and propulsion time. The obtained best-fit parameters are $\epsilon = 0.023$ and $\tau_0 = 0.27$. Note that τ_0 is close to the previous estimations. Figures 5*b* and 7 show the obtained best fit compared to the data set. We further added the optimal pattern for the limit case $\epsilon = 0$. For this case, the model predicts the intuitive opposition mode (IdC = 0) as the optimal pattern of coordination. Indeed, if there is no benefit to glide ($\epsilon \leq 0$), then the swimmer should not glide.

The model shows that there exists a single optimal coordination (here $\text{IdC}_c \approx -17\%$) for non-dimensional velocity lower than $u_c = 0.82$. The swimmers would save $\approx 0.5\%$ energy and control their speed by varying their force ($\varphi < 1$). They do not use the maximum force per stroke consistently with the observations of Craig & Pendergast [7]. The present model provides a physical explanation to these observations. Above this critical velocity, the swimmers use their maximum force per stroke and hence follow the maximum force model presented before. The model captures the sudden change in the index of coordination evolution with speed and links it to a physical argument.

(d) Linear approximation and two regimes

It is interesting to note that in equations (4.7)–(4.8), we can define $X = u_-/\sqrt{\varphi}$ and write all the parameters as a function of X only. Therefore, $\mathcal{R}$ is a function of X only.

To linearize the equations developed in the two previous subsections, we will assume $\tau_0 \ll 1$ and $\epsilon \ll 1$. We further assume that $\epsilon \ll \tau_0$. Keeping only the smallest order terms in ϵ and τ_0, it comes

$$\mathcal{R}_{\mathrm{cu}}(X) \approx 1 - \epsilon\left(1 - X^2\right) + \frac{{\tau_0}^2}{2}\left(\frac{1+X^4}{2X^2} - 1\right). \tag{4.15}$$

This approximated function has a single minimum in $X \in [0,1]$

$$X_0 = \frac{1}{\left(1 + 4\epsilon/\tau_0^2\right)^{1/4}}, \tag{4.16}$$

and its value is

$$\mathcal{R}_{\mathrm{cu}}^{\min} = 1 - \epsilon + \frac{\tau_0^2}{2}\left(\sqrt{1 + \frac{4\epsilon}{\tau_0^2}} - 1\right). \tag{4.17}$$

Injecting this expression in the evaluation of the index of coordination and keeping only the first-order term, it comes that the optimal index of coordination is

$$\mathrm{IdC}_c \approx -\frac{1}{2}\left(1 - \frac{1}{\sqrt{1 + 4\epsilon/\tau_0^2}}\right). \tag{4.18}$$

This will be the optimal choice of coordination as long as $\overline{u} < (1 + 2\mathrm{IdC}_c)^{1/2}$. Above the critical speed

$$u_c \approx \frac{1}{\left(1 + 4\epsilon/\tau_0^2\right)^{1/4}}, \tag{4.19}$$

the swimmers will then be in the maximum force regime.

From equation (4.18), we observe that the absolute value of the optimal index of coordination increases (decreases) when ϵ (τ_0) increases. It is not surprising to expect that the swimmer will tend to glide more when ϵ increases. Note that if $\epsilon = 0$, then the expression yields that the optimal coordination is the opposition mode ($\mathrm{IdC} = 0$). The effect of varying τ_0 is maybe less obvious. Increasing τ_0 (keeping all the other parameters constant) can be compared to swimming with paddles. This will increase the parameter α_h in equation (4.13). From the present model, we then expect the swimmers to change their coordination pattern towards the opposition mode (IdC closer to zero) with paddles. This prediction is observed by Sidney *et al.* [30].

In all the results, presented so far, the legs were tied and could not be used by the swimmers. It is rather clear that allowing the legs to kick will lead to an increase of the swimmer characteristic velocity v^*. This will affect the non-dimensional propulsion time τ_0. If we suppose that the legs do not affect the gliding effectiveness ϵ and drag coefficient k_b and that the physical propulsion time is the same, the coordination is then affected by an apparent reduction of τ_0. This would lead to a decrease of the absolute value of the IdC_c (towards the opposition). We further discuss this point in appendix C.

5. Conclusion and applications

In the present paper, we report the evolution of arm coordination patterns in front-crawl with velocities of expert swimmers and studied this evolution theoretically. We propose that swimmers change their mode of coordination to minimize their energy consumption at a given velocity. They chose a constant negative index of coordination at low velocity and vary their speed with the force they use per stroke. This is a stroke with alternated propulsion and gliding pauses. The constant index corresponds to a fix repartition of propulsion and recovery with velocity. Above a critical velocity, swimmers use a maximum force regime and start reducing

the gliding time to further increase their velocity. The index of coordination increases till the characteristic velocity $v^* = \overline{v}_{\max}/\sqrt{1 + 2\mathrm{IdC}_{\max}}$. Above this velocity, the pattern of coordination becomes a superposition mode typical of elite sprinters. The burst-and-coast approach presented in the §4 shows the advantage of catch-up mode and captures the change of evolution of the arm-organization with velocity.

Using the model presented here, we believe it is possible to advise on individual optimal arm coordination for each swimmer based on his/her physical characteristics. The swimmers are characterized by three parameters in the burst-and-coast approach: the characteristic velocity v^*, the propulsion time τ_0 and their gliding effectiveness coefficient $\epsilon > 0$. This model could also be applied to swimmers with disabilities and advise them on individual optimal arm coordination based on their physical characteristics and type of impairment. Extension to other strokes are possible and should be considered in future work.

The present approach could be interesting to the study of other modes of locomotion in Nature. For instance, walking can be seen as a superposition mode on land, where two feet touch the ground at the same time for an extended duration of time. Running on the other hand is closer to a catch-up mode, with a period of time with no ground contact. Surprisingly, in this case, the change is reversed. A similar approach to the one presented here could provide new insight to this challenging question of walk to run transition.

Ethics. All the athletes volunteered for this study and gave their written consent to participate.

Data accessibility. The experimental data presented are accessible in the electronic supplementary material.

Authors' contributions. L.S. and D.C. collected the data. R.C. and C.C. analysed the data and proposed the model description. R.C. drafted the manuscript. All authors gave final approval for submission.

Competing interests. We have no competing interests.

Funding. No funding has been received for this article.

Acknowledgements. The authors thank all the athletes that participated in the tests. They are also grateful to Leo Chabert, Benoit Bideau, Jeremy Kalfoun, Charlie Pretot and Vincent Bacot for their help at different stages of the project and the useful discussions. The authors appreciated the useful comments and suggestions of the reviewer to improve the quality of the paper. Last but not least, the authors thank The Olympic Multimedia Library for granting us access to the footage of the race and allowing us to use the images to illustrate our work.

Appendix A. Error evaluation

The error bars in the figures of the present paper take into account the propagation of error in their analysis. This appendix aims at clarifying their calculations. The absolute error on the index of coordination is $\sigma_{\mathrm{IdC}} = 3\%$ [15]. For the velocity measurement, the error is estimated to be $\sigma_{\overline{v}} = 0.01\overline{v}$.

For the rest, we use the propagation of error formula. Consider, for example, the calculated parameter $\mathcal{F}(x_1, x_2, \ldots, x_n)$, where $\{x_i\}_{i=1,2,\ldots n}$ are some parameters with uncertainties $\{\sigma_{x_i}\}_{i=1,2,\ldots n}$ known or calculated previously. Then the uncertainty on $\mathcal{F}$ can be estimated by

$$\sigma_{\mathcal{F}}^2 = \sum_{i=1}^{n} \sigma_{x_i}^2 \left| \frac{\partial \mathcal{F}}{\partial x_i} \right|^2. \tag{A 1}$$

We assume here that all the parameters are always un-correlated. For instance, the characteristic velocity v^* is calculated using equation (3.6). The error on v^* is then

$$\sigma_{v^*}^2 = \sigma_{\mathrm{IdC}}^2 \frac{\overline{v}_{\max}^2}{(1 + 2\mathrm{IdC}_{\max})^3} + \sigma_{\overline{v}_{\max}}^2 \frac{1}{(1 + 2 * \mathrm{IdC}_{\max})}. \tag{A 2}$$

When the swimmers' data are grouped per velocity, the data are averaged on $n_{\mathcal{G}}$ points of the group $\mathcal{G}$. The velocity, index of coordination and propulsion time are computed as

$$a_{\mathcal{G}} = \frac{1}{n_{\mathcal{G}}} \sum_{i=1\cdots n_{\mathcal{G}}} a_i, \tag{A 3}$$

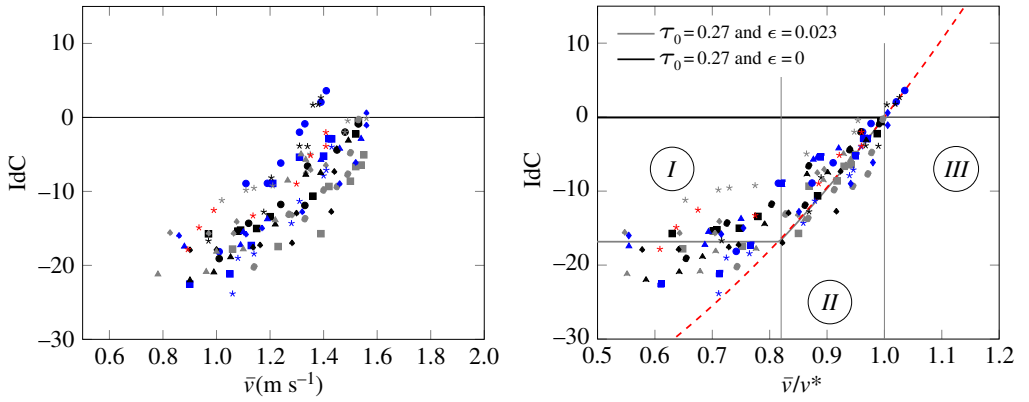

Figure 8. Arm coordination with the velocity for the 16 swimmers separately. Each symbol represents a single swimmer. The dashed line corresponds to the maximum force model while the solid lines show the result of the model presented in the paper for the parameters listed. (Online version in colour.)

and the error is estimated as

$$\sigma^2_{a_\mathcal{G}} = \frac{1}{n^2_\mathcal{G}} \sum_{i=1\cdots n_\mathcal{G}} \sigma^2_{a_i} + \left(\sigma^{std}_{a_\mathcal{G}}\right)^2, \tag{A 4}$$

where the first term accounts for the propagation of error of the averaging and the second one to the standard deviation of the measurement of the $n_\mathcal{G}$ swimmers. This second term aims at capturing the variability among the swimmers.

Appendix B. Index of coordination of the 16 swimmers

We provide here the raw data for all the swimmers for the index of coordination with dimensional velocity and after applying the evaluation of the characteristic speed $v^* = \overline{v}_{\max}/\sqrt{1 + 2\mathrm{IdC}_{\max}}$, where $\overline{v}_{\max}$ denotes the maximum velocity achieved by the swimmer. The results are displayed in figure 8.

Appendix C. Impact of the legs kicking on the coordination

Throughout the paper, the legs were tied. In previous works done by Chollet *et al.* [9] and Seifert *et al.* [10], the swimmers were allowed to used their legs. The velocities the swimmers could reach were larger by 20% compared to the present one for similar level swimmers. In this appendix we look at other data taken on similar level swimmers with the legs free to kick. We did not measure the resistance coefficient for these swimmers with the MAD-system. They only performed the coordination test.

We applied the same analysis as done in the present paper to the data of velocity and coordination. The results are displayed in figure 9 and compared to the swimmers with no legs of the present paper. We observe a similar trend. The swimmers select a constant index of coordination at low velocity and then follow the maximum force model. The characteristic velocity v^* increased from 1.5 m s^{-1} without leg to 1.8 m s^{-1} with legs on average.

At low velocity, the swimmers usually perform one kick per arm stroke and at higher velocity up to three [31]. We will assume it is linked to the force choice of the arms and also in phase. Then the effect of the legs can be either a reduction of the effective drag k_b or an increase of the propulsion force T_a. In all cases, it will lead to an increase of the characteristic velocity v^* and the coordination is certainly affected by this.

In this appendix, we will assume it is only the thrust that is increased and therefore the drag is of the same magnitude ($k_b = 30$ kg m^{-1}). Then if the physical propulsion time is the same, the

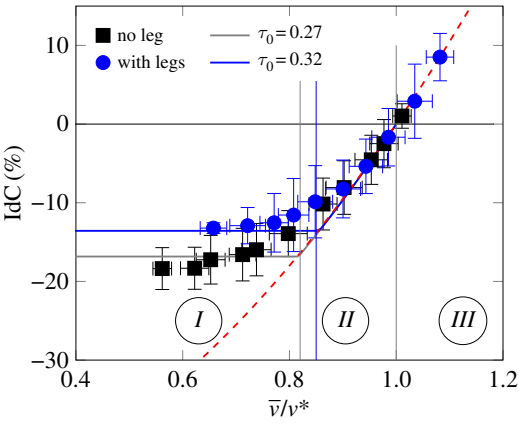

Figure 9. Arm coordination with the mean non-dimensional velocity for swimmers with and without legs. The dashed line corresponds to the maximum force model. The solid lines show the optimal coordination with $\tau_0 = 0.27$ and $\tau_{0,\dagger} = 0.401$ in grey and blue, respectively. In both cases, we used $\epsilon = 0.023$. (Online version in colour.)

non-dimensional one should be rescaled $\tau_{0,\dagger} = \tau_0 v^*_\dagger / v^*$, where the † indicates the quantity with the legs free to kick. Using τ_0 without leg the value found previously, we get $\tau_{0,\dagger} = 0.32$ with legs. Our model then will predict for a similar ϵ an increase of the index of coordination from −17% to −12%. This is in good agreement with the observations.

References

1. Villa P, Soriano S, Pollarolo L, Smriglio C, Gaeta M, D'Orazio M, Conforti J, Tozzi C. 2020 Neandertals on the beach: use of marine resources at Grotta dei Moscerini (Latium, Italy). *PLoS ONE* **15**, 1–35. (doi:10.1371/journal.pone.0226690)
2. Verhaegen M, Munro S. 2011 Pachyosteosclerosis suggests archaic Homo frequently collected sessile littoral foods. *Homo* **62**, 237–247. (doi:10.1016/j.jchb.2011.06.002)
3. Trinkaus E, Samsel M, Villotte S. 2019 External auditory exostoses among western Eurasian late Middle and Late Pleistocene humans. *PLoS ONE* **14**, e0220464. (doi:10.1371/journal.pone.0220464)
4. McVicar JW. 1936 A brief history of the development of swimming. *Res. Q. Am. Phys. Educ. Assoc.* **7**, 56–67. (doi:10.1080/23267402.1936.10761757)
5. Barbosa TM, Bragada JA, Reis VM, Marinho DA, Carvalho C, Silva AJ. 2010 Energetics and biomechanics as determining factors of swimming performance: updating the state of the art. *J. Sci. Med. Sport* **13**, 262–269. (doi:10.1016/j.jsams.2009.01.003)
6. Craig AB, Skehan PL, Pawelczyk JA, Boomer WL. 1985 Velocity, stroke rate, and distance per stroke during elite swimming competition. *Med. Sci. Sports Exerc.* **17**, 625–634. (doi:10.1249/00005768-198512000-00001)
7. Craig AB, Pendergast DR. 1979 Relationships of stroke rate, distance per stroke, and velocity in competitive swimming. *Med. Sci. Sports* **11**, 278–283. (doi:10.1249/00005768-197901130-00011)
8. Costill DL, Maglischo EW, Richardson AB. 1992 *Swimming*. Oxford, UK: Blackwell Scientific Publications.
9. Chollet D, Chalies S, Chatard J. 2000 A new index of coordination for the crawl: description and usefulness. *Int. J. Sports Med.* **21**, 54–59. (doi:10.1055/s-2000-8855)
10. Seifert L, Chollet D, Rouard A. 2007 Swimming constraints and arm coordination. *Hum. Mov. Sci.* **26**, 68–86. (doi:10.1016/j.humov.2006.09.003)
11. Ericsson KA, Lehmann AC. 1996 Expert and exceptional performance: evidence of maximal adaptation to task constraints. *Annu. Rev. Psychol.* **47**, 273–305. (doi:10.1146/annurev.psych.47.1.273)
12. Truijens M, Toussaint H. 2005 Biomechanical aspects of peak performance in human swimming. *Anim. Biol.* **55**, 17–40. (doi:10.1163/1570756053276907)

13. Toussaint H, De Groot G, Savelberg H, Vervoorn K, Hollander A, van Ingen Schenau G. 1988 Active drag related to velocity in male and female swimmers. *J. Biomech.* **21**, 435–438. (doi:10.1016/0021-9290(88)90149-2)
14. Seifert L, Toussaint H, Alberty M, Schnitzler C, Chollet D. 2010 Arm coordination, power, and swim efficiency in national and regional front crawl swimmers. *Hum. Mov. Sci.* **29**, 426–439. (doi:10.1016/j.humov.2009.11.003)
15. Seifert L, Schnitzler C, Aujouannet Y, Carter M, Rouard A, Chollet D. 2006 Comparison of subjective and objective methods of determination of stroke phases to analyse arm coordination in front-crawl. *Port. J. Sport Sci.* **6** (Supl. 2), 92–94.
16. Matsuda Y, Yamada Y, Ikuta Y, Nomura T, Oda S. 2014 Intracyclic velocity variation and arm coordination for different skilled swimmers in the front crawl. *J. Hum. Kinet.* **44**, 67–74. (doi:10.2478/hukin-2014-0111)
17. Bideault G, Herault R, Seifert L. 2013 Data modelling reveals inter-individual variability of front crawl swimming. *J. Sci. Med. Sport* **16**, 281–285. (doi:10.1016/j.jsams.2012.08.001)
18. Seifert L, Chollet D, Bardy B. 2004 Effect of swimming velocity on arm coordination in the front crawl: a dynamic analysis. *J. Sports Sci.* **22**, 651–660. (doi:10.1080/02640410310001655787)
19. Figueiredo P, Toussaint HM, Vilas-Boas JP, Fernandes RJ. 2013a Relation between efficiency and energy cost with coordination in aquatic locomotion. *Eur. J. Appl. Physiol.* **113**, 651–659. (doi:10.1007/s00421-012-2468-8)
20. Figueiredo P, Morais P, Vilas-Boas JP, Fernandes RJ. 2013b Changes in arm coordination and stroke parameters on transition through the lactate threshold. *Eur. J. Appl. Physiol.* **113**, 1957–1964. (doi:10.1007/s00421-013-2617-8)
21. Videler J, Weihs D. 1982 Energetic advantages of burst-and-coast swimming of fish at high speeds. *J. Exp. Biol.* **97**, 169–178.
22. Bulgakova N, Makarenko L. 1966 Sport Swimming. Physical Culture, Education and Science. Moscow. Russian State Academy of Physical Education.
23. Caspersen C, Berthelsen PA, Eik M, Pâkozdi C, Kjendlie PL. 2010 Added mass in human swimmers: age and gender differences. *J. Biomech.* **43**, 2369–2373. (doi:10.1016/j.jbiomech.2010.04.022)
24. Klauck J, Ungerechts B. 2014 The determinationof'added mass' of swimmers as a part of studies of non-steady flow patterns. *BMS 2014-Proc*.
25. Martin RB, Yeater RA, White MK. 1981 A simple analytical model for the crawl stroke. *J. Biomech.* **14**, 539–548. (doi:10.1016/0021-9290(81)90003-8)
26. Zamparo P, Pendergast D, Mollendorf J, Termin A, Minetti A. 2005 An energy balance of front crawl. *Eur. J. Appl. Physiol.* **94**, 134–144. (doi:10.1007/s00421-004-1281-4)
27. van Houwelingen J, Willemsen D, Kunnen R, van Heijst G, Grift E, Breugem W, Delfos R, Westerweel J, Clercx H, van de Water W. 2017 The effect of finger spreading on drag of the hand in human swimming. *J. Biomech.* **63**, 67–73. (doi:10.1016/j.jbiomech.2017.08.002)
28. Powell MJ. 1964 An efficient method for finding the minimum of a function of several variables without calculating derivatives. *Comput. J.* **7**, 155–162. (doi:10.1093/comjnl/7.2.155)
29. Kiefer J. 1953 Sequential minimax search for a maximum. *Proc. Am. Math. Soc.* **4**, 502–506. (doi:10.1090/S0002-9939-1953-0055639-3)
30. Sidney M, Paillette S, Hespel J, Chollet D, Pelayo P. 2001 Effect of swim paddles on the intra-cyclic velocity variations and on the arm coordination of front crawl stroke. In *ISBS-Conf. Proc. Archive* vol. 1.
31. Millet G, Chollet D, Chalies S, Chatard J. 2002 Coordination in front crawl in elite triathletes and elite swimmers. *Int. J. Sports Med.* **23**, 99–104. (doi:10.1055/s-2002-20126)